LDA+*U* and tight-binding electronic structure of InN nanowires

A. Molina-Sánchez, A. García-Cristóbal, and A. Cantarero
Instituto de Ciencia de Materiales, Universidad de Valencia, E-46071 Valencia, Spain

A. Terentjevs
Physics Department, Politecnico of Torino, Torino, Italy

G. Cicero
Chemistry and Materials Science Engineering Department, Politecnico of Torino, Torino, Italy
(Received 30 July 2010; published 20 October 2010)

In this paper we employ a combined *ab initio* and tight-binding approach to obtain the electronic and optical properties of hydrogenated Indium nitride (InN) nanowires. We first discuss InN band structure for the wurtzite structure calculated at the LDA+*U* level and use this information to extract the parameters needed for an empirical tight-binging implementation. These parameters are then employed to calculate the electronic and optical properties of InN nanowires in a diameter range that would not be affordable by *ab initio* techniques. The reliability of the large nanowires results is assessed by explicitly comparing the electronic structure of a small diameter wire studied both at LDA+*U* and tight-binding level.

DOI: 10.1103/PhysRevB.82.165324 PACS number(s): 71.15.Mb, 73.22.Dj, 78.20.Bh, 73.21.Hb

I. INTRODUCTION

Indium nitride (InN) has received considerable attention in recent years due to its direct band gap in the infrared range[1,2] and the high electron mobilities.[3] The possibility of fabricating low-dimensional structures such as nanowires (NWs) (Refs. 4 and 5) makes desirable the simulation of the electronic structure and optical properties of these system with atomistic approaches. *Ab initio*-based calculations are, in principle, capable of reproducing the band structure of bulk and systems of few atoms with a great accuracy. However, the computational time turns out to be a limiting factor if the number of atoms increases, making this methods impractical for the study of dependencies with the size and composition (alloying) of the system. However, the valuable *ab initio* information can be used for the development of empirical tight-binding (TB) (Ref. 6) or pseudopotential[7] methods. These approaches are expected to describe with good precision the optical properties of both bulk and small systems, and at the same time, to allow quantitative studies of large systems in reasonable computational times. Moreover, as opposed to the approaches based on the effective mass approximation (EMA), the empirical atomistic methods are able to incorporate the true symmetry of the nanostructures.[8]

Ab initio methods have been widely employed for the study of InN (see, e.g., Refs. 9 and 10). In particular, it has been shown that in order to get a correct description of its band structure close to the Γ point within the density-functional theory (DFT) it is important to repair the deficiency of local-density approximation (LDA) or generalized gradient approximation (GGA) functional in describing the Coulomb interaction between the localized *d* electrons of Indium. To this end, various approaches have been built on the DFT basis and, among others we mention the self-interaction correction methods[11,12] and the LDA with the Hubbard *U* correction (LDA+*U*).[13,14] In our work, we adopt an LDA+*U* approach, which has been recently discussed and applied to the case of InN.[15] Beyond DFT calculations, the GW methods provides good estimation of the nitrides band gap, opening it up the experimental value. However, this method is computationally more complex than LDA+*U*, making difficult its application in large systems.[16,17]

Among the various empirical approaches, we have chosen to work with the tight-binding method, that has demonstrated its applicability in III-N nanowires.[18] Moreover, this method allows to deal easily with the problem of the dangling bonds at the free surface of the nanowires,[19] and gives an intuitive physical picture of the wave functions in terms of the atomic orbitals. The TB parameters are obtained by fitting the LDA+*U* bulk band structure to some selected points of the Brillouin zone, with special care in a faithful description of the neighborhood of the top of the valence band because of its dominant role in the determination of the optical properties.

Since there is no *a priori* guaranty of the transferability of the fitted TB parameters for their use in nanostructures calculations, we have compared the band structure of a small InN nanowire (diameter 16.2 Å) calculated with the LDA+*U* and TB approaches, and obtain a very good agreement. The use of this empirical tight-binding model in larger InN nanowires has been illustrated by calculating the dependence of the confinement energy on the NW size and the polarization dependence optical spectra for a nanowire size beyond the range accessible by *ab initio* calculations.

II. INDIUM NITRIDE BULK

InN has been studied by employing DFT-LDA (Ref. 20) calculations with on-site Hubbard *U* correction (LDA+*U*), using ultrasoft pseudopotentials as realized in QUANTUM ESPRESSO,[21] and expanding the electronic wave functions in plane waves. To describe correctly the structural properties of InN, the 4*d* electrons of the Indium are explicitly consid-

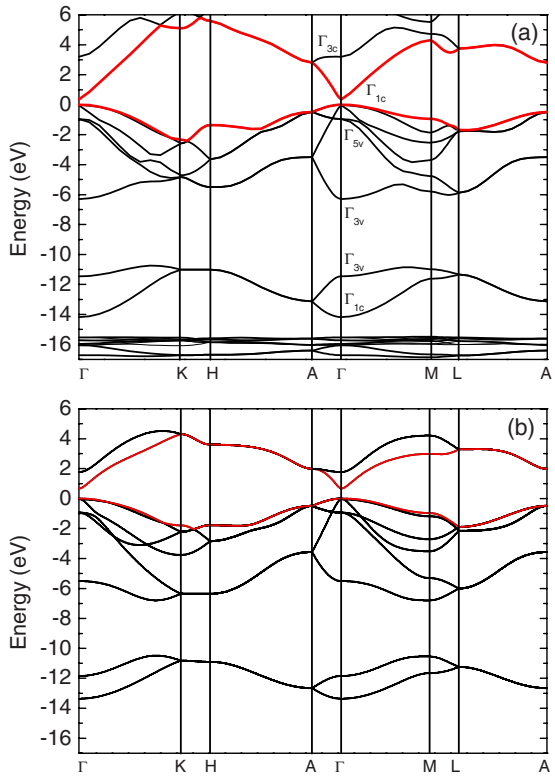

FIG. 1. (Color online) Band structure of InN bulk obtained with (a) LDA+U and (b) TB approaches. The symmetry group labels of some relevant states are indicated in (a).

ered as valence electrons.[22] For all calculations, the plane wave cutoff is 30 Ry, and a $(8\times8\times8)$ Monkhorst-Pack mesh is used.

It is known that LDA and GGA underestimate the binding energy of the cation semicore d states and overestimate their hybridization with the anion p valence states. As a result, an artificially large p-d coupling pushes up the valence band maximum (VBM) reducing the calculated band gap; in particular, in the case of InN, DFT-LDA gives null or negative band gap [the experimental band gap is ~0.67 eV (Refs. 2 and 23)]. In this work we use the LDA+U (Refs. 13, 14, and 24) method to correct this deficiency. To describe correctly the main InN band features, we have applied the U correction both to indium 4d electrons and to nitrogen 2p electrons. We note that in the case of InN, similarly to some oxides compounds,[25] the inclusion of the U correction on the anion (the N p-shell) is important for a better description of p-d interaction and, besides inducing the band gap opening, it gives the correct symmetry of the states close to the top of the valence band. The spin-orbit interaction is not taken into account in these calculations. The selected U parameters are U_d=6.0 eV for In, U_p=1.5 eV for N, as discussed in details elsewhere.[15] Within this computational scheme, we obtained equilibrium lattice parameters for InN bulk in the wurtzite structure of a=3.505 Å, c/a=1.616, and u=0.378. These values are close to the experimental data [a=3.538 Å, c/a =1.612, and u=0.377 (Ref. 26)]. In Fig. 1(a) the band structure for the InN bulk is presented: the band gap at Γ is 0.34 eV, the valence band width is about 6.3 eV and the 4d indium states lie 16 eV below the VBM. The band gap becomes positive but it is still underestimated as compared with the experimental value. Another remarkable improvement with respect to LDA consists of the correct description of the energy-level ordering and symmetry at the top of the valence band, which are essential to derive reliable TB parameters.

Concerning the empirical TB method, we have selected a basis of four orbital per atom, s,p_x,p_y,p_z (sp^3 model), as described in Refs. 27. It is known that a better description of the conduction bands far from the Γ point would require at least the use of an sp^3s^*.[28] However, we will focus our study in the optical properties near Γ, and to keep the number of fitting parameters reduced, we avoid the addition of the s^* excited orbital. As we only include interaction between nearest neighbors, the crystal-field splitting at the top of the valence band cannot be reproduced since this is an effect caused by the interaction with second and third neighbors. This limitation is corrected by the introduction of one *ad hoc* asymmetry between p_x-p_y and p_z orbitals.[29] Moreover, the deviation from the ideal wurtzite has been introduced with the Harrison's rule, applied to the interatomic parameters[30]

$$V(d) = \left(\frac{d_0}{d}\right)^{\eta} V(d_0), \tag{1}$$

where d is the relaxed LDA+U distance, d_0 the ideal wurtzite distance, and η an exponent that depends on the orbital. In most of the literature, the accepted value for the exponent is around 2,[31] although some authors make a discretionary use of such exponents in order to obtain a good description of the band structure under deformation (see Ref. 32) or a better agreement over the whole Brillouin zone (see in Ref. 33). In an attempt to limit the number of additional parameters we restrict the η to be different only for the overlap $s-p_z$. A optimized set of TB parameters fitted with this procedure against the LDA+U band structure is shown in Table

TABLE I. TB parameters (in electron volt) of InN proposed in this work. We follow the standard TB notation also used in Ref. 27.

E_s^c	E_p^c	E_s^a	E_p^a	$E_{p_z}^a$	η
−5.5247	9.6179	−6.7910	0.0461	−0.0076	1.8
$V_{ss\sigma}$	$V_{s_cp_a}$	$V_{s_ap_c}$	$V_{pp\sigma}$	$V_{pp\pi}$	$\eta_{s,p_z,\sigma}$
−1.7500	2.5981	−0.1083	−1.3000	3.0700	2.5

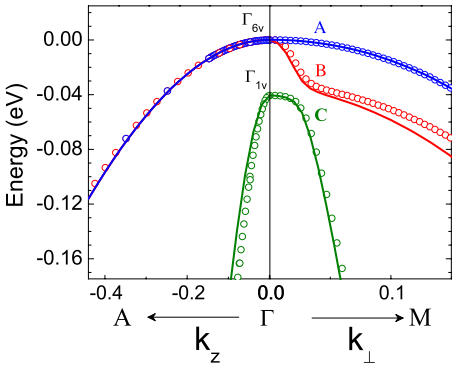

FIG. 2. (Color online) Top of the InN valence band. The empty circles correspond to the LDA+U bands, and the lines represent the TB bands. The component k_z of the wave vector $\boldsymbol{k}$ is normalized to $\frac{\pi}{c}$, such that $k_z=1$ correspond to A. The wave vector in the M direction is expressed as $\frac{\pi}{a}(\xi,\frac{1}{\sqrt{3}}\xi,0)$, where $0\leq\xi\leq1$. The symmetry group of the states at Γ are indicated and the bands are denoted as A, B, and C.

I, and the corresponding TB band structure is represented in Fig. 1(b). Nevertheless, the band gap has been fixed to the experimental value.[1] The obtained valence band reproduces well the LDA+U results. The discrepancies at around −6 eV below the top of the valence band are attributed to the small basis set used in the sp^3 TB method.[27]

In Fig. 2 we report the details of the top of the valence band at Γ, comparing LDA+U (open circles) with TB calculations (lines), along the ΓA and ΓM directions. We observe a very accurate fitting for the A-C bands whereas the B-band shows a slight deviation for $k>0.1$ in the M direction. Along the ΓA direction, A and B bands are degenerate and both calculations match perfectly. The anticrossing between B and C bands is also well captured by the TB method. The TB effective mass of the top of the valence band at Γ are $m_\perp^A=2.80$, $m_z^A=1.86$, $m_\perp^B=0.07$, $m_z^B=1.86$, $m_\perp^C=0.57$, and $m_z^C=0.07$. Regarding the symmetry of the wave functions at Γ,[34] the degenerate states belong to the representation Γ_{6v}. They have a pure composition of p_x and p_y orbitals, that coincides with both LDA+U and TB results. The second state in energy belongs to the representation Γ_{1v}, being here 100% p_z for both calculations. Note that the bottom of the conduction band state also belongs to this representation, although the predominant orbital is in this case s type. The TB conduction effective masses are $m_\perp^c=0.07$ and $m_z^c=0.08$, in agreement with the data of Ref. 35. The achieved good agreement at Γ is of special relevance for the eventual use of the TB band structure in the analysis of optical and transport experiments.

III. INDIUM NITRIDE NANOWIRES

To asses the behavior of the TB parametrization in nanostructures, a comparison between the electronic states, calculated with LDA+U and TB approaches, has been performed, for a thin NW. Afterwards, a study in larger NWs with the TB method has been carried out, by exploring the band gap evolution with the NWs diameter and examining the optical response for a selected diameter.

The nanowire employed in the comparison has a diameter of 16.2 Å (see sketch in the left upper part of Fig. 3), and the dangling bonds at the free surfaces are passivated with hydrogen atoms in order to avoid the presence of surface states within the gap.[36] In the *ab initio* calculation, the nanowire structure has been fully optimized until forces on atoms are less than 0.001 Ry/bohr per atom. We use a Monkhorst-Pack mesh of 6 points for the one dimensional nanowire Brillouin zone. The indium and nitrogen atoms placed at the surface

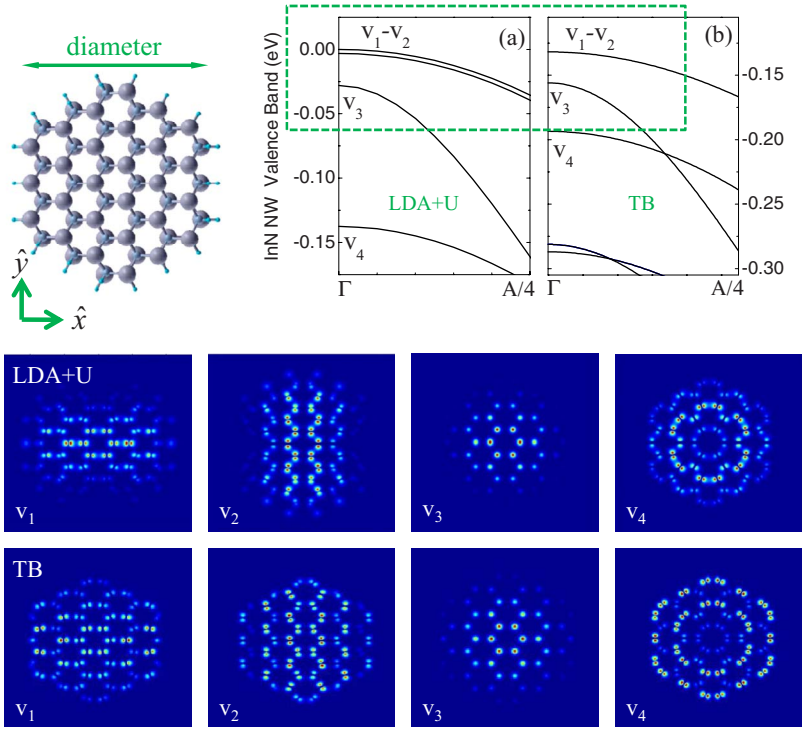

FIG. 3. (Color online) In the left upper part, nanowire represented with ball-and-sticks of diameter 16.2 Å. As well in the upper part, top of the valence band calculated with (a) LDAU and (b) TB method. In the lower part, we represent the square of the wave function for the valence band states v_1, v_2, v_3, and v_4 calculated with both approaches.

modify slightly its tetragonal bond due to the presence of the passivant hydrogen atoms, changing slightly their interatomic distances. This surface reconstruction is not taken into account in the TB calculation, which assumes a perfect wurtzite everywhere.[37] The topmost valence band states, labeled in increasing energy as $v_1, v_2, \ldots$, are shown in Fig. 3 [(a) LDA+U and (b) TB method]. The states v_1 to v_4 are within a range of 150 meV in both calculation. The TB result yields in addition the value of −130 meV for the confinement energy of the states v_1 and v_2 with respect to the top of bulk valence band. In the case of the LDA+U calculation, the degeneracy between v_1 and v_2 is broken due to the exact consideration of the atomic distances when we relax the structure, an effect that the TB method ignores (such splitting has the small value of 3 meV). In any case, the portion of the band structure framed by a dashed green line, that contains the v_1, v_2, and v_3 subbands, exhibit a remarkable similarity in both calculations. In particular, the curvature of the bands are identical and only a slight difference between the v_1 and v_3 states (26 meV and 18 meV for LDA+U and TB calculation, respectively) is observed. Concerning the v_4 state, one can perceive that is closer in energy to v_3 in the TB calculations than in the LDA+U approximation. Despite that energy is underestimated, v_4 has the same curvature in both approaches. Another difference between both methods is the existence of more states in the range of −150 meV from the state v_1, in the case of TB valence band. In order to exclude the relaxation as a source of error in our comparison, calculations with LDA+U in a nanowire, assuming perfect wurtzite everywhere were performed, without finding any substantial difference.

In the lower part of Fig. 3 we show the square of the Γ wave function, $\langle \Psi | \Psi \rangle$, for the valence band states, v_1 to v_4. The TB wave function can be expressed as

$$\Psi_\Gamma(\boldsymbol{r}) = \sum_{\alpha,j} A_{\alpha,j} \phi_j(\boldsymbol{r} - \boldsymbol{r}_{\boldsymbol{\alpha}}) \tag{2}$$

here the index α runs over atoms and j over orbitals. For the sake of simplicity, the orbitals are represented here with the hydrogen wave functions that share the same symmetry.[38] Fig. 3 shows that the density is localized on the indium and nitrogen atoms, without spreading on the hydrogen atoms. The first two degenerate valence band states (v_1 and v_2) exhibit the electron density elongated along two perpendicular directions (x and y). Moreover, by looking closely to the density of each atom, it is evident that it comes from the p_x and p_y orbitals, for the x-elongated (v_1) and y-elongated (v_2) states, respectively. In the next valence band state, v_3, the wave function is notably confined at the center of the NW, being the p_z-orbital component predominant. In the case of the v_4 state, we find that the wave function has a node in the nanowire center, and a mixed composition of $p_x - p_y$ orbitals. One can distinguish that TB charge densities are more delocalized toward the NW surface if compared to the LDA+U picture. Even so, TB method reproduces exactly the qualitative features of the charge density in terms of symmetry and orbital composition. The observed differences are acceptable because of the restricted TB basis and the small sizes of the NW. For larger NWs, these small differences between the TB method and the LDA+U approximation are expected to be attenuated. We thus conclude that the TB parameters obtained and tested here are suitable to be used in the calculation of optical properties of InN-based nanostructures.

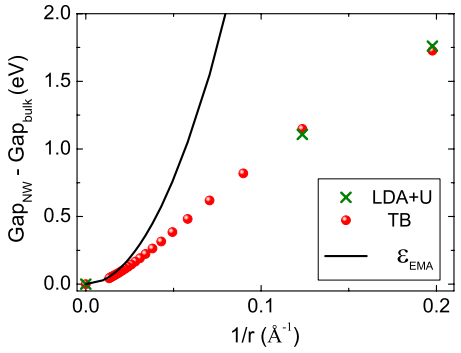

FIG. 4. (Color online) Dependence of the confinement energy on the nanowire size. The limit of $1/r \to 0$ is the bulk band gap.

Once demonstrated the reliability of the TB approach and the quality of the parameters, we have performed TB calculations for larger NWs. In the first place, we show in Fig. 4 the confinement energy, defined as the difference between the nanowire and bulk band gap, versus $1/r$, being r the NW radius. The full circles correspond to the TB results and the band gap energies calculated with LDA+U for two NWs are drawn with full rectangles. The confinement energy calculated with the effective mass approximation, assuming parabolic bands, is

$$\varepsilon_{\mathrm{EMA}} = \left(\frac{\hbar^2}{2m_\perp^c} + \frac{\hbar^2}{2m_\perp^A} \right) \left(\frac{k_1^0}{r} \right)^2, \tag{3}$$

$k_1^0 = 2.4048$, being the first zero of the Bessel function $J_0(x)$, and the effective masses are reported in Sec. II. For large radii, when $1/r < 0.03$ Å^{-1}, the TB method and the EMA follow the same trend, proportional to $1/r^2$. For decreasing radii ($1/r > 0.03$ Å^{-1}) EMA overestimate the confinement energy as compared with the TB results, that changes in this range the $\sim 1/r^2$ behavior to $\sim 1/r$. Moreover, the TB results connect perfectly with the *ab initio* computed values, represented by full squares, at radii 8.1 and 5.1 Å. This smooth interpolation confirms the suitability of the TB method to link the NWs size ranges of 10 Å, where *ab initio* are practical and 100 Å, where the (EMA) start to be applicable. In this intermediate size range the TB approach has the advantages of keeping the atomistic nature of the system and be efficient in terms of computational effort.

In addition the TB method offers the possibility of calculating the optical absorption spectra without introducing new parameters in the model. The absorption coefficient for light with polarization vector $\boldsymbol{e}$ can be written as[39]

$$\alpha^e(\hbar\omega) \propto \int_{BZ} f_{c,v}^e(k)\, \delta(E_{c,k} - E_{v,k} - \hbar\omega), \tag{4}$$

where we integrate over the one-dimensional Brillouin zone, and the oscillator strength is calculated as

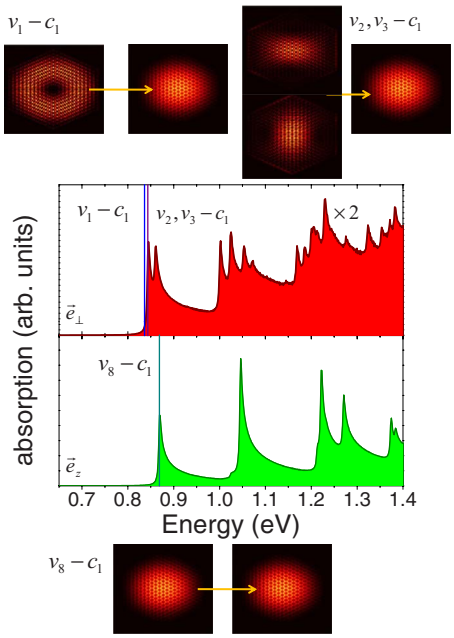

FIG. 5. (Color online) Optical absorption spectra for in-plane ($\boldsymbol{e}_\perp$ multiplied by two) and on-axis ($\boldsymbol{e}_z$) light polarization (see main text). The wave functions that participate in the relevant optical transitions are also represented (both spectra are displayed in the same scale).

$$f^{\boldsymbol{e}}_{c,v}(k) \propto \frac{|\langle \Psi_c | \boldsymbol{e} \cdot \boldsymbol{p} | \Psi_v \rangle|^2}{E_{c,k} - E_{v,k}}. \tag{5}$$

The momentum matrix element, $\langle \Psi_c | \boldsymbol{e} \cdot \boldsymbol{p} | \Psi_v \rangle$, is calculated as in Ref. 40, for two light polarizations: in-plane (perpendicular to NW axis), $\boldsymbol{e}_\perp = 1/\sqrt{2}(\hat{x} + i\hat{y})$, and in-axis (parallel to NW axis), $\boldsymbol{e}_z = \hat{z}$. The delta function is replaced by a Lorentz function of width 7 meV. In Fig. 5 we represent the absorption spectrum of a NW of diameter 70.8 Å for the defined light polarizations. The valence and conduction wave functions that participate in the transitions at the absorption edge are also shown. In both spectra it is recognized the one-dimensional density of states (modulated by the oscillator strength), the $\boldsymbol{e}_z$ spectra exhibiting a larger separation between the absorption peaks. By analyzing more in more detail the $\boldsymbol{e}_\perp$ spectra, one can appreciate that absorption edge does not take place at the energy of the fundamental band gap (corresponding to the transition $v_1 - c_1$). This is because the symmetry valence state v_1 (see Fig. 5), whose charge density has a node in the at the NW center, making negligible the spatial overlap between the states v_1 and c_1. The first optically active transition, blueshifted 10 meV with respect to the fundamental gap, involves the degenerate states v_2 and v_3, shown in Fig. 5. On the other hand, the absorption edge of the $\boldsymbol{e}_z$ spectra is shifted 24 meV with respect the $\boldsymbol{e}_\perp$ spectra since the first state with significant p_z orbital component is v_8.

IV. CONCLUSIONS

In this work, we have obtained an InN band structure with a fundamental band gap of 0.34 eV, by means of LDA+U calculations. The Hubbard U correction to the d orbitals of indium and p orbitals of nitrogen has palliated the zero band gap problem of InN, present in LDA or GGA calculations. The LDA+U band structure has been fitted with a sp^3 tight-binding model obtaining a very reasonable overall agreement despite the small size of the TB basis. It is specially noticeable the satisfactory coincidence between the energy and symmetry of the wave functions at Γ point.

This fitted set of TB parameters is, in principle, usable for calculations of the electronic structure of quantum wells, wires or/and dots. In order to test the suitability of this empirical approach, a band-structure calculation is performed of a InN NW of 16.2 Å diameter and compare with the corresponding LDA+U calculation, which includes a previous relaxation of the atomic positions. This comparison shows that, without any additional fitting, the TB band structure and wave functions matches adequately with their *ab initio* counterparts. Possibly, the remaining differences between the two models could be reduced by employing a TB model with an extended orbital basis set, although this would increase the number of parameters and computational time. The study the evolution of the NW band gap with the radius confirms the adequacy of TB method to connect efficiently very small sizes nanoobjects (a few angstrom) accessible with *ab initio* approaches, with large sizes nanostructures (hundreds of angstrom), where continuous methods are commonly employed. Finally, the potential of this empirical atomistic approach is illustrated by the analysis of the absorption of a large nanowire.

ACKNOWLEDGMENTS

This work has been supported by the NANOLICHT project (NanoSci-ERA) and the Ministry of Science and Innovation (under Grant No. MAT2009-10350). Computer time was provided by CINECA through the CNR-INFM "Iniziativa Calcolo Parallelo" and by Tirant Supercomputer of the Red Española de Supercomputación (RES), hosted in the University of Valencia.

[1] V. Y. Davydov, A. A. Klochikhin, R. P. Seisyan, V. V. Emtsev, S. V. Ivanov, F. Bechstedt, J. Furthmüller, H. Harima, A. V. Mudryi, J. Aderhold, O. Semchinova, and J. Graul, Phys. Status Solidi B **229**, R1 (2002).

[2] J. Wu, W. Walukiewicz, K. M. Yu, J. W. Ager III, E. E. Haller, H. Lu, W. J. Schaff, Y. Saito, and Y. Nanishi, Appl. Phys. Lett. **80**, 3967 (2002).

[3] W. Walukiewicz, J. W. Ager III, K. M. Yu, Z. Liliental-Weber, J. Wu, S. X. Li, R. E. Jones, and J. D. Denlinger, J. Phys. D **39**, R83 (2006).

[4] E. Calleja, J. Ristic, S. Fernandez-Garrido, L. Ceruffi, M. A. Sánchez-García, J. Grandal, A. Trampert, U. Jahn, G. Sánchez, A. Griol, and B. Sánchez, Phys. Status Solidi B **244**, 2816 (2007).
[5] B. Pal, K. Goto, M. Ikezawa, Y. Masumoto, P. Mohan, J. Motohisa, and T. Fukui, Appl. Phys. Lett. **93**, 073105 (2008).
[6] A. Di Carlo, Semicond. Sci. Technol. **18**, R1 (2003).
[7] G. Bester, J. Phys.: Condens. Matter **21**, 023202 (2009).
[8] G. Bester and A. Zunger, Phys. Rev. B **71**, 045318 (2005).
[9] C. Stampfl and C. G. Van de Walle, Phys. Rev. B **59**, 5521 (1999).
[10] J. Furthmüller, P. H. Hahn, F. Fuchs, and F. Bechstedt, Phys. Rev. B **72**, 205106 (2005).
[11] M. M. Rieger and P. Vogl, Phys. Rev. B **52**, 16567 (1995).
[12] D. Vogel, P. Krüger, and J. Pollmann, Phys. Rev. B **55**, 12836 (1997).
[13] V. I. Anisimov, F. Aryasetiawan, and A. I. Lichtenstein, J. Phys.: Condens. Matter **9**, 767 (1997).
[14] M. Cococcioni and S. de Gironcoli, Phys. Rev. B **71**, 035105 (2005).
[15] A. Terentjevs, A. Catellani, D. Prendergast, and G. Cicero, Phys. Rev. B **82**, 165307 (2010).
[16] P. Rinke, M. Winkelnkemper, A. Qteish, D. Bimberg, J. Neugebauer, and M. Scheffler, Phys. Rev. B **77**, 075202 (2008).
[17] A. Svane, N. E. Christensen, I. Gorczcyca, M. van Schilfgaarde, A. N. Chantis, and T. Kotani, Phys. Rev. B **82**, 115102 (2010).
[18] D. Camacho Mojica and Y. M. Niquet, Phys. Rev. B **81**, 195313 (2010).
[19] Y. M. Niquet, C. Delerue, G. Allan, and M. Lannoo, Phys. Rev. B **62**, 5109 (2000).
[20] J. P. Perdew and A. Zunger, Phys. Rev. B **23**, 5048 (1981).
[21] P. Giannozzi, S. Baroni, N. Bonini, M. Calandra, R. Car, C. Cavazzoni, D. Ceresoli, G. L. Chiarotti, M. Cococcioni, I. Dabo, A. Dal Corso, S. de Gironcoli, S. Fabris, G. Fratesi, R. Gebauer, U. Gerstmann, C. Gougoussis, A. Kokalj, M. Lazzeri, L. Martin-Samos, N. Marzari, F. Mauri, R. Mazzarello, S. Paolini, A. Pasquarello, L. Paulatto, C. Sbraccia, S. Scandolo, G. Sclauzero, A. P. Seitsonen, A. Smogunov, P. Umari, and R. M. Wentzcovitch, J. Phys.: Condens. Matter **21**, 395502 (2009).
[22] A. F. Wright and J. S. Nelson, Phys. Rev. B **51**, 7866 (1995).
[23] J. S. Thakur, Y. V. Danylyuk, D. Haddad, V. M. Naik, R. Naik, and G. W. Auner, Phys. Rev. B **76**, 035309 (2007).
[24] A. Janotti, D. Segev, and C. G. Van de Walle, Phys. Rev. B **74**, 045202 (2006).
[25] M. Korotin, T. Fujiwara, and V. Anisimov, Phys. Rev. B **62**, 5696 (2000).
[26] W. Paszkowicz, R. Cerný, and S. Krukowski, Powder Diffr. **18**, 114 (2003).
[27] A. Kobayashi, O. F. Sankey, S. M. Volz, and J. D. Dow, Phys. Rev. B **28**, 935 (1983).
[28] P. Vogl, H. P. Hjalmarson, and J. D. Dow, J. Phys. Chem. Solids **44**, 365 (1983).
[29] S. Schulz, S. Schumacher, and G. Czycholl, Eur. Phys. J. B **64**, 51 (2008).
[30] W. A. Harrison, *Electronic Structure and the Properties of Solids* (Dover, New York, 1989).
[31] G. H. Li, A. R. Goñi, C. Abraham, K. Syassen, P. V. Santos, A. Cantarero, O. Brandt, and K. Ploog, Phys. Rev. B **50**, 1575 (1994).
[32] T. B. Boykin, G. Klimeck, R. C. Bowen, and F. Oyafuso, Phys. Rev. B **66**, 125207 (2002).
[33] J. Jancu, F. Bassani, F. D. Sala, and R. Scholz, Appl. Phys. Lett. **81**, 4838 (2002).
[34] L. C. Lew Yan Voon, M. Willatzen, M. Cardona, and N. E. Christensen, Phys. Rev. B **53**, 10703 (1996).
[35] J. Wu, J. Appl. Phys. **106**, 011101 (2009).
[36] X. Huang, E. Lindgren, and J. R. Chelikowsky, Phys. Rev. B **71**, 165328 (2005).
[37] M. P. Persson and A. Di Carlo, J. Appl. Phys. **104**, 073718 (2008).
[38] A. Galindo and P. Pascual, *Quantum Mechanics I* (Springer-Verlag, Berlin, 1990).
[39] M. Virgilio and G. Grosso, Phys. Rev. B **77**, 165315 (2008).
[40] L. C. Lew Yan Voon and L. R. Ram-Mohan, Phys. Rev. B **47**, 15500 (1993).